

# Critical Current in Various Pinning Landscapes

Andreas Glatz<sup>1</sup>, Igor Aronson<sup>1</sup>, George Crabtree<sup>1</sup>, Alexei Koshelev<sup>1</sup>, Ivan Sadovsky<sup>1</sup>, Dmitry Karpeev<sup>2</sup>, Carolyn Phillips<sup>2</sup>

<sup>1</sup>Materials Science Science Division, Argonne National Laboratory, Argonne, IL 60439, USA

<sup>2</sup>Mathematics and Computer Division, Argonne National Laboratory, Argonne, IL 60439, USA

## GL model & Motivation

### Time-dependent Ginzburg-Landau

TDGL equations: 
$$\frac{\partial \Psi}{\partial t} = -\frac{\delta \mathcal{F}_{GL}}{\delta \Psi^*}, \quad \frac{\delta \mathcal{F}_{GL}}{\delta \mathbf{A}} = 0$$

In dimensionless units:

$$u(\partial_t + i\mu)\psi = \epsilon(\mathbf{r})\psi - |\psi|^2\psi + (\nabla - i\mathbf{A})^2\psi + \zeta(\mathbf{r}, t)$$

$$\kappa^2 \nabla \times (\nabla \times \mathbf{A}) = \mathbf{J}_n + \mathbf{J}_s + \mathcal{I}$$

Coupled system for  $\psi$  and  $\mathbf{A}$ :  
 $\psi$ : complex order parameter characterizing density of Cooper pairs  
 $\mathbf{A}$ : vector potential for magnetic field  
 $\zeta$  and  $\mathcal{I}$ : thermal fluctuations  
 $\epsilon(\mathbf{r}) = \frac{T_c(\mathbf{r}) - T}{T_c} \rightarrow 0$  for  $T \rightarrow T_c$  (critical temperature)

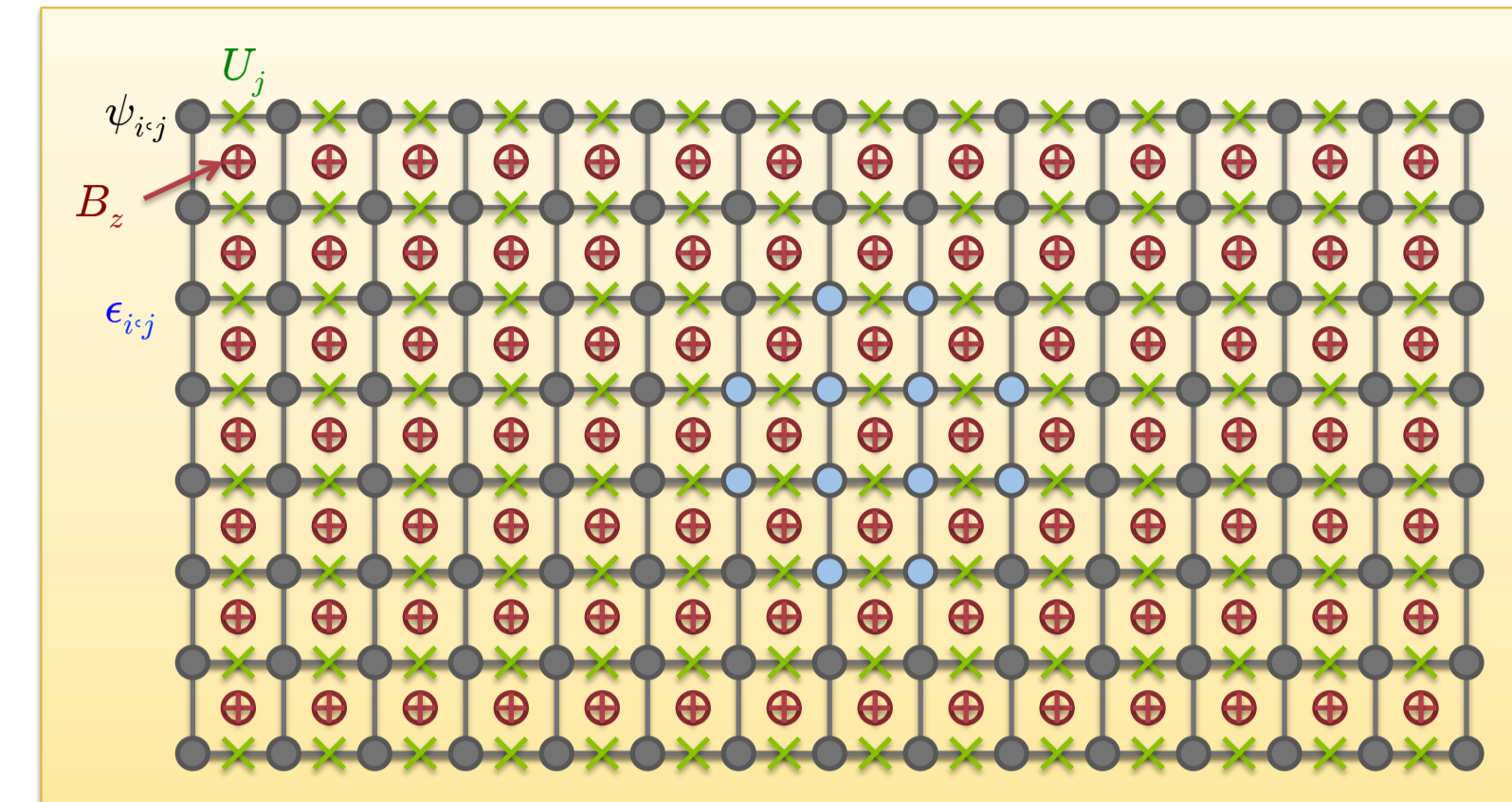
Total current:  $\mathbf{J} = \mathbf{J}_s + \mathbf{J}_n$       $\mathbf{J} = \text{Im}[\psi^*(\nabla - i\mathbf{A})\psi] - (\nabla\mu + \partial_t\mathbf{A})$

### OSCon: Robust optimization of pinning & geometry for high critical currents and resulting energy applications

- Critical current determined by long-time evolution of TDGL (to stationary flow)
- Dominated by rare events of vortex depinning, avalanches, nucleation and splitting & reconnection
- Frequency and duration of pinning/depinning depends on configurations of inclusions
- Suitable pinning configurations must be determined using geometry optimization

## Modeling of pinning

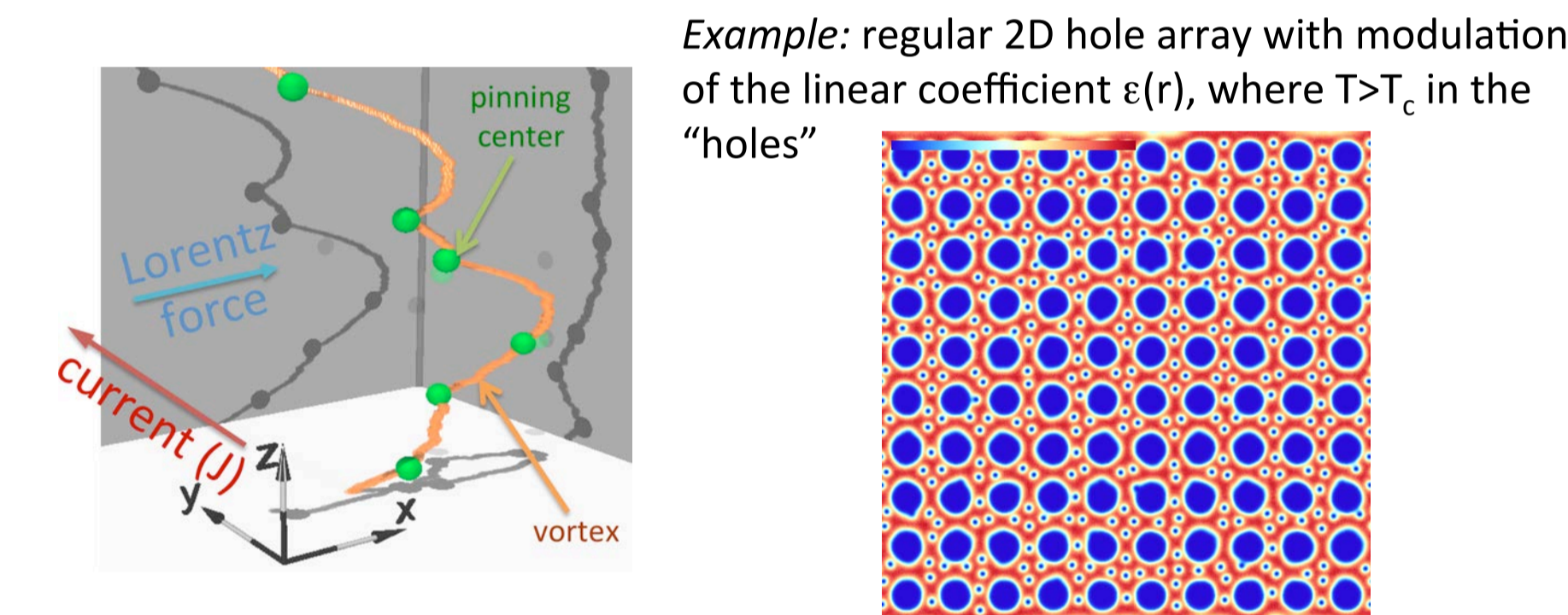
### Here: Regular simulation grid (on GPUs)



### T<sub>c</sub> modulation: Inclusions and pinning

Inclusions and defects are modeled by T<sub>c</sub> modulation → corresponding to normal metallic pinning centers: spatial variation of  $\epsilon(\mathbf{r})$  [positive in the superconductor, negative in the defect]

- arbitrary geometry
- on a regular grid

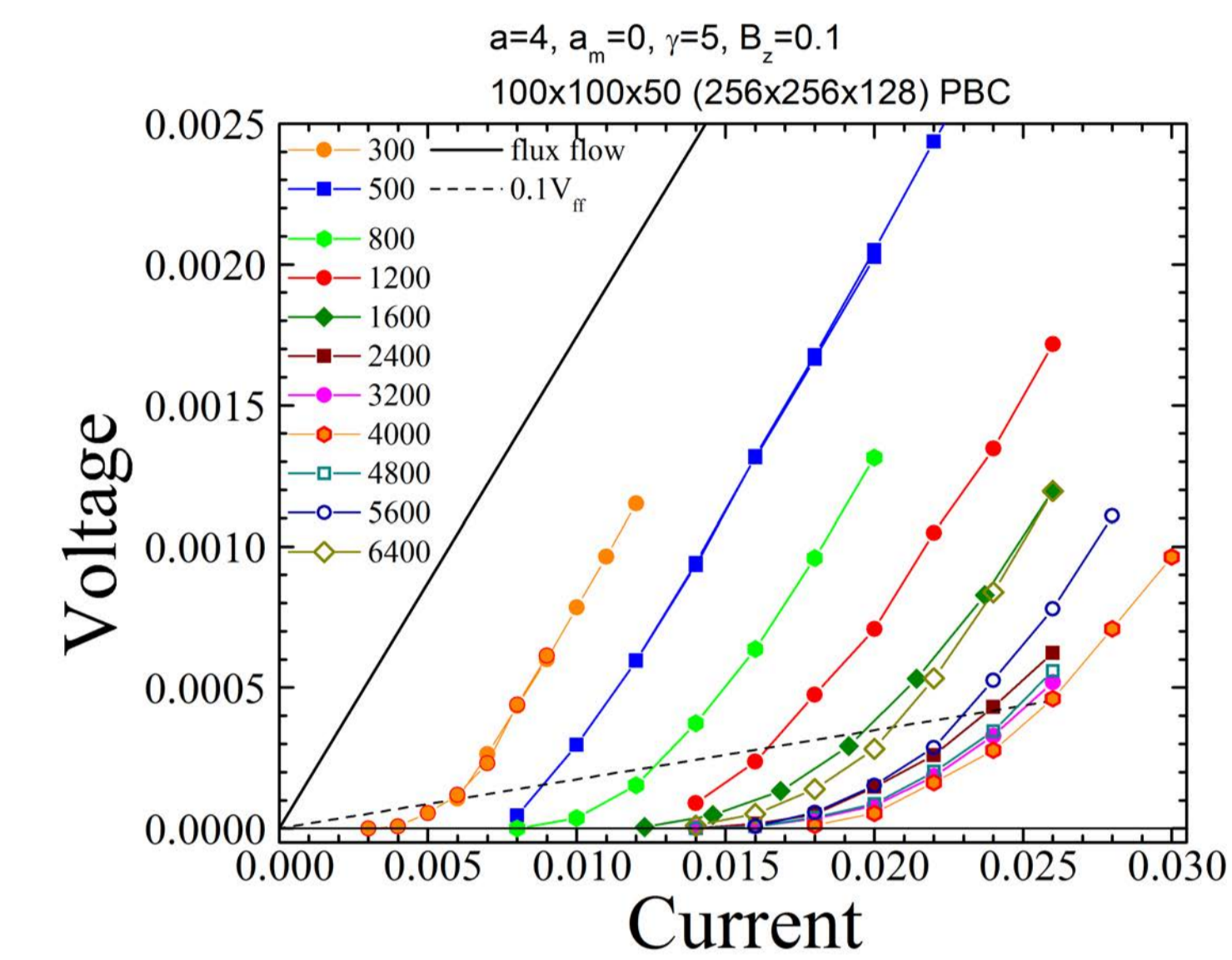


## Random spherical inclusions

2<sup>nd</sup> type of inclusions: insulators → modeled by zero-normal-supercurrent boundary conditions

- Most appropriate on unstructured meshes (see poster 2)
- On regular meshes normal to mesh edges (in progress)

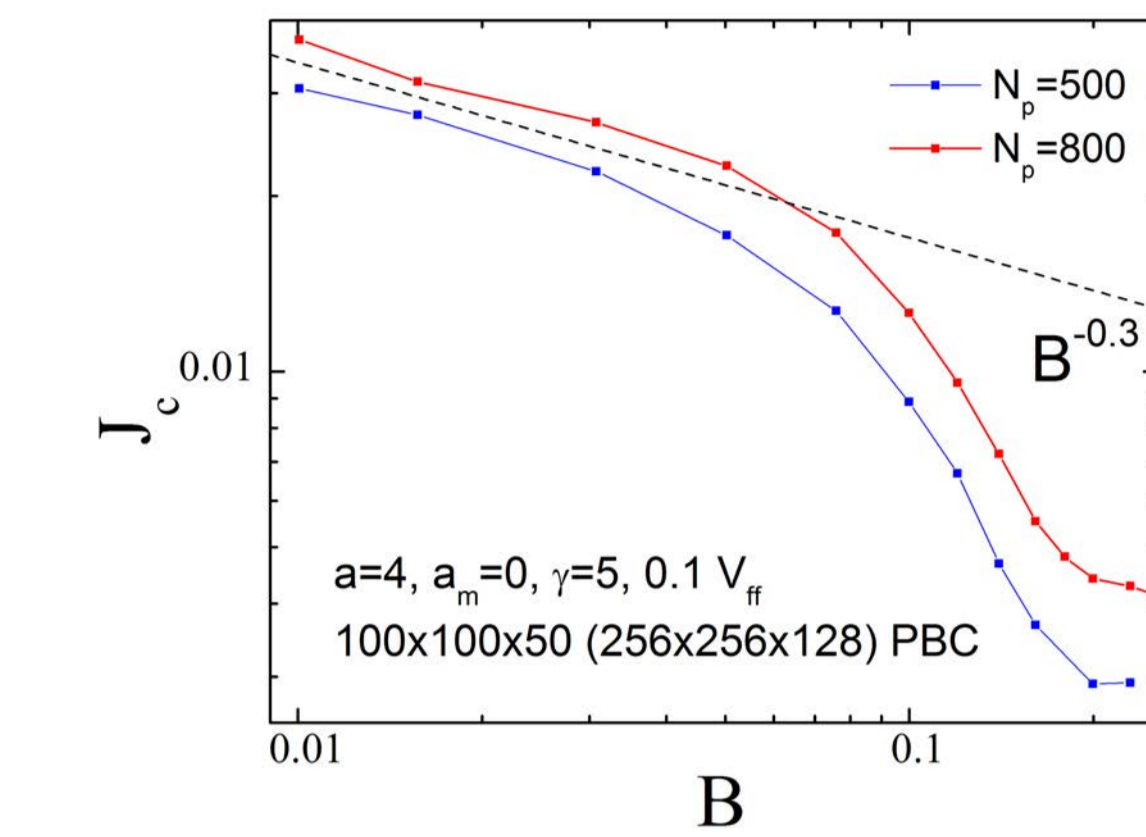
### Critical currents for spherical (metallic) inclusions



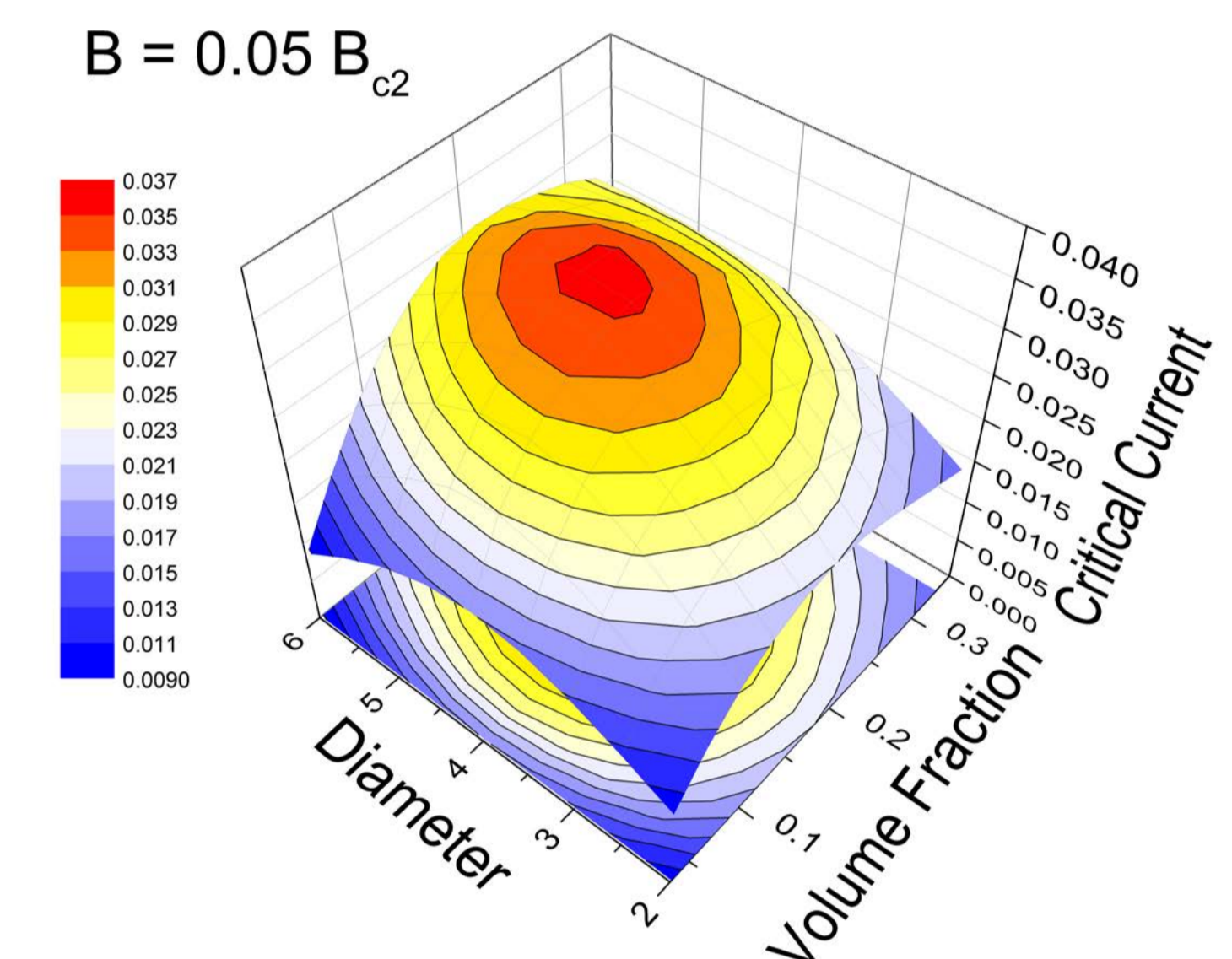
Current-voltage characteristics for different inclusion concentrations (inclusions are randomly distributed in the simulation volume: the critical current is determined by a fraction of the corresponding free flux flow voltage)

Instead of the concentration, the volume fraction and inclusion diameter are the two parameters characterizing the random spherical pinning landscape.

Critical current also depends on magnetic field:

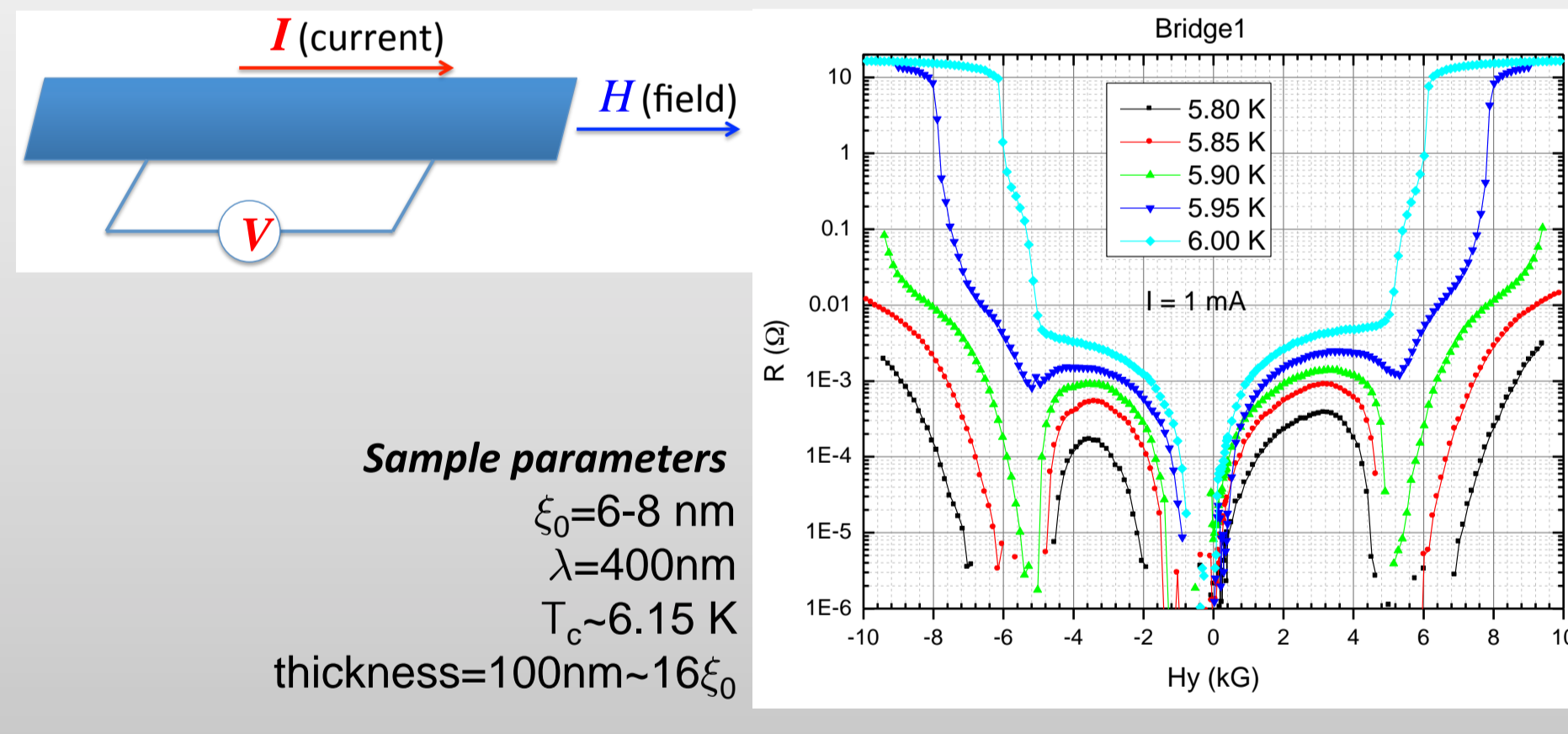


### Optimal critical current



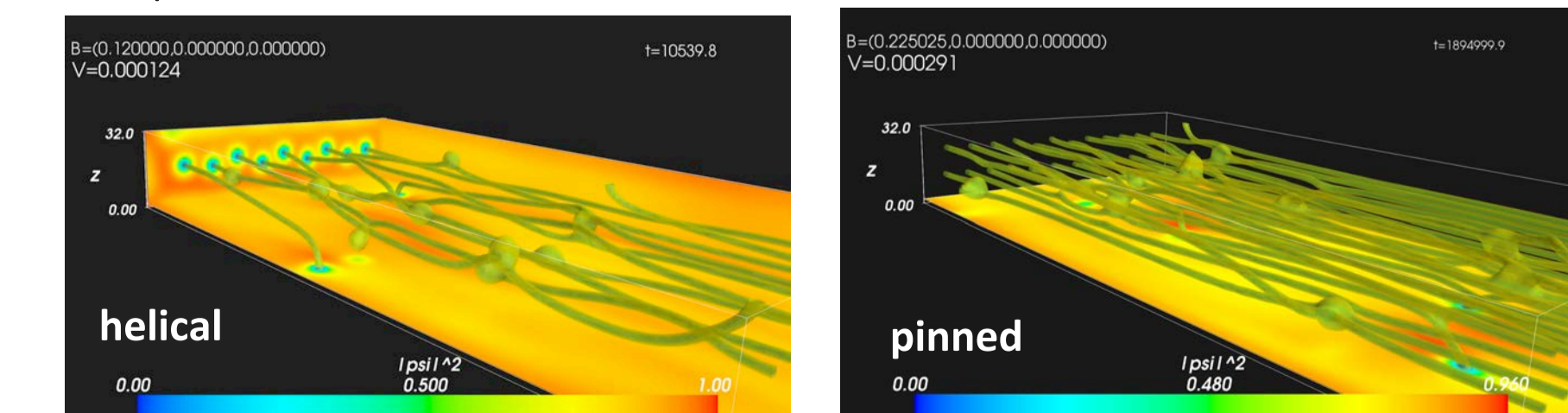
## Parallel fields

### Experimental result: MoGe slab with parallel current and field



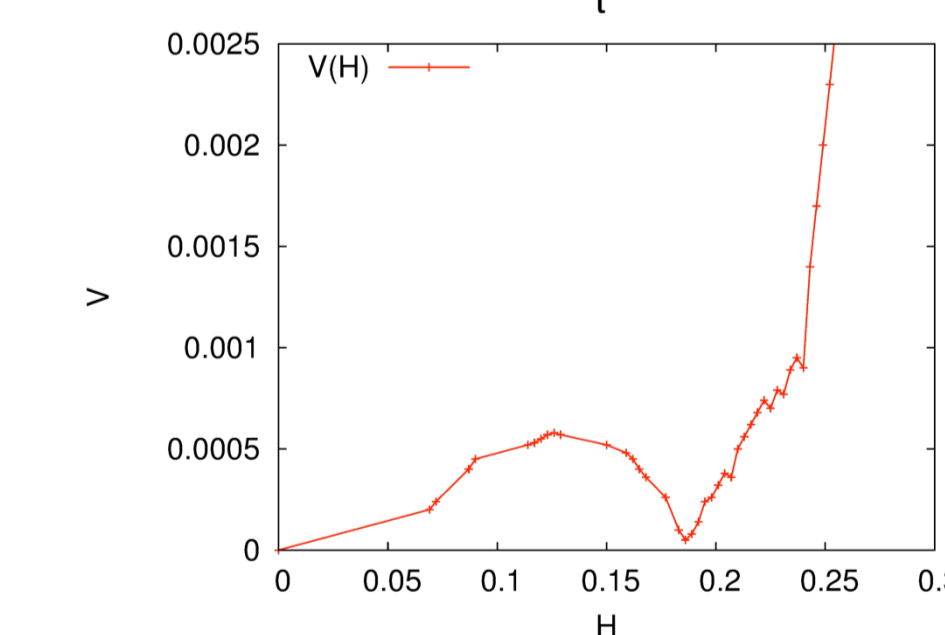
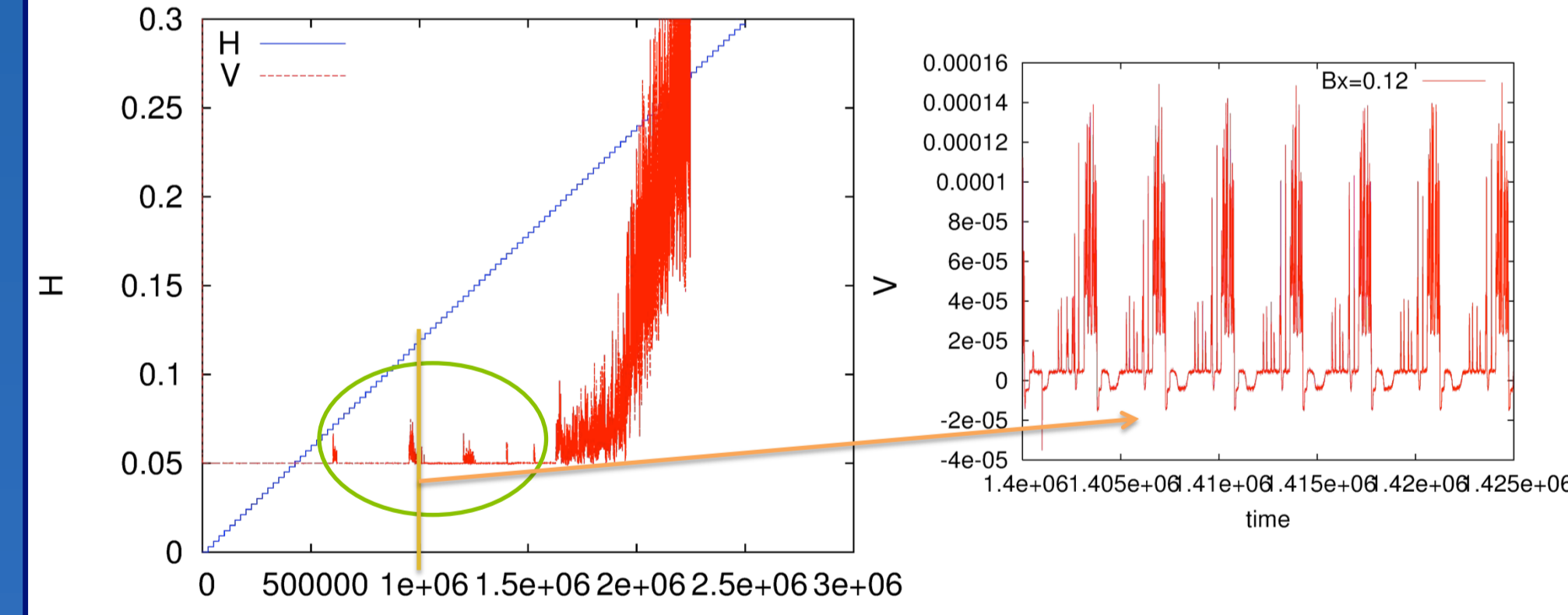
### Numerical realization

- Sample is discretized using a regular mesh of 512x128x32 grid points with mesh size of  $\xi_0/2$  → realistic thickness
- Sample is periodic in x-direction
- Inclusions are modeled by a different low-T<sub>c</sub> component
- 0-100 spherical inclusions with diameter  $5\xi_0$  are randomly placed in the volume → average over different disorder realizations
- A fixed constant current is applied in x-direction as well as a variable magnetic field
- Simulation time: 25mill time steps for 100 field values



### Helical motion & Reentrance

Magnetic field & voltage for one disorder configuration



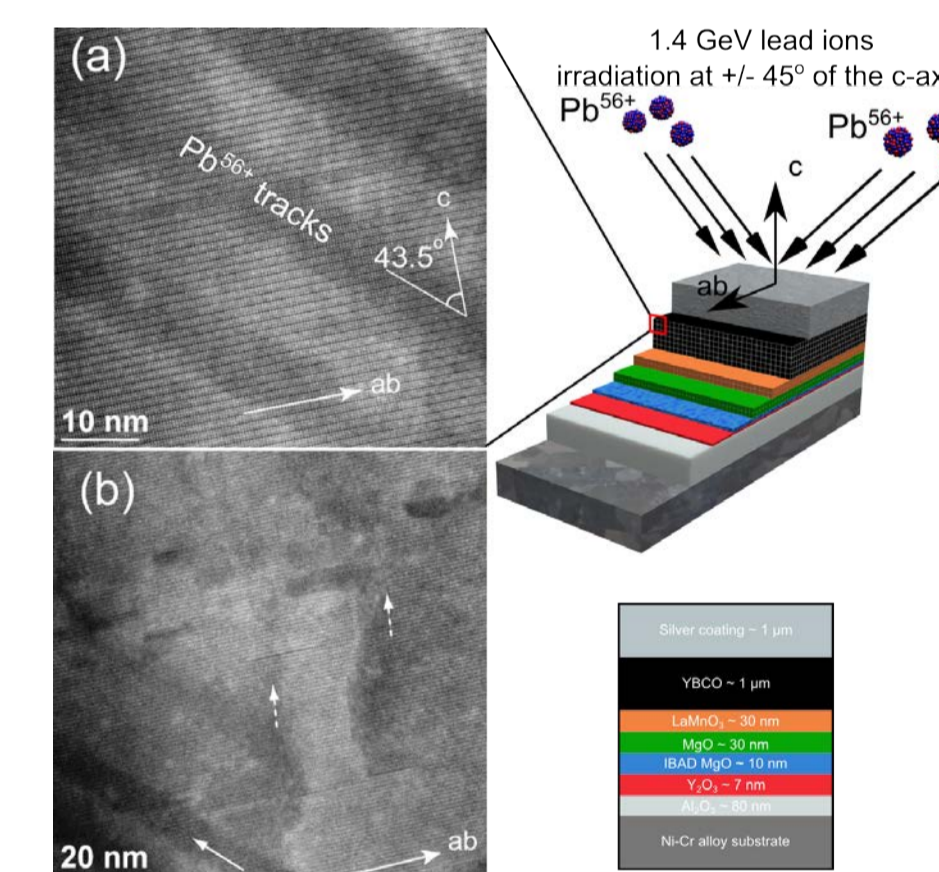
- Magnetic field applied in parallel to the applied current:
- No Lorentz force if vortices are straight
  - Source for instabilities: impurities or thermal fluctuations
  - Dense vortex lines help to "re-stabilize" the vortex lattice

**New discovery:** a new periodically "rotating" vortex state appears at intermediate field strength having finite resistance

Visualization using location of inclusions and vortex detection results (see poster 3)

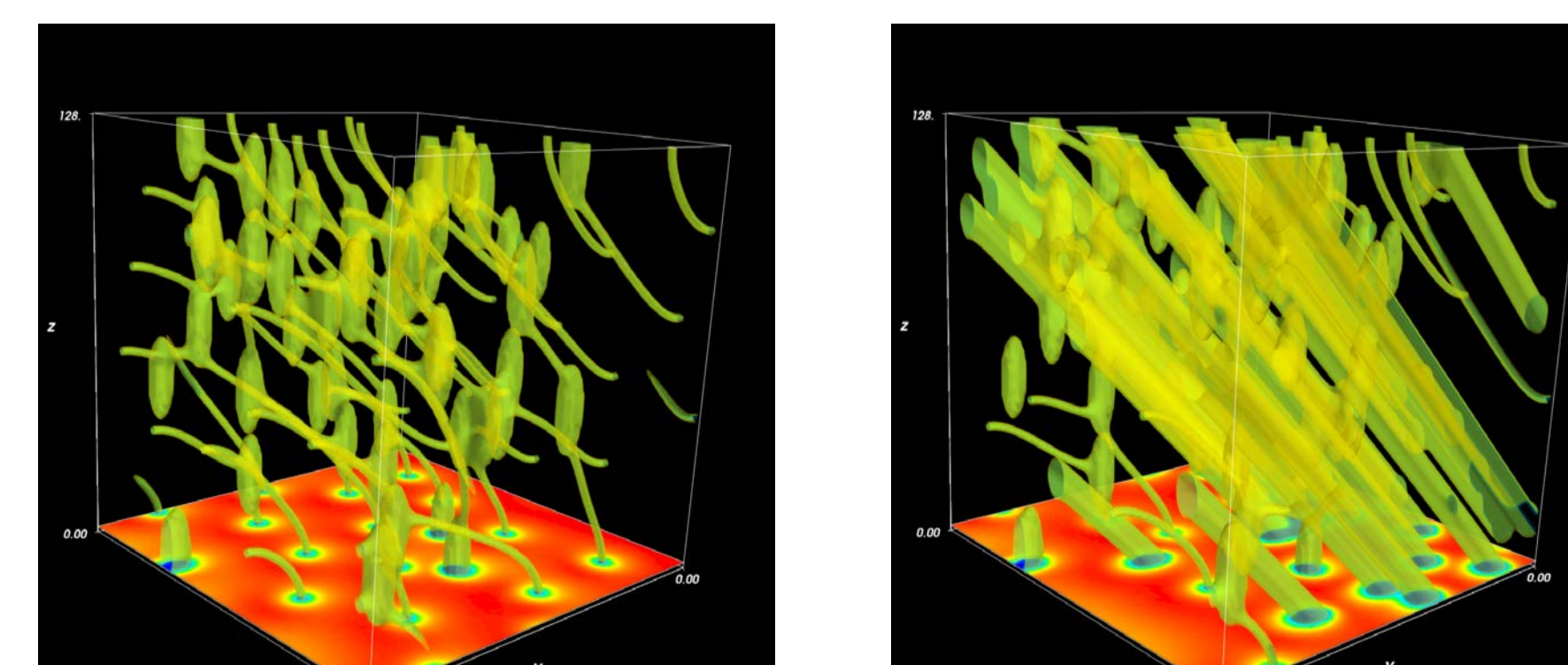


## Competing defects



Commercial superconducting tape with nanorod inclusions is irradiated by heavy ions at 45 deg → understanding of the critical current depending on the angle of the external magnetic field

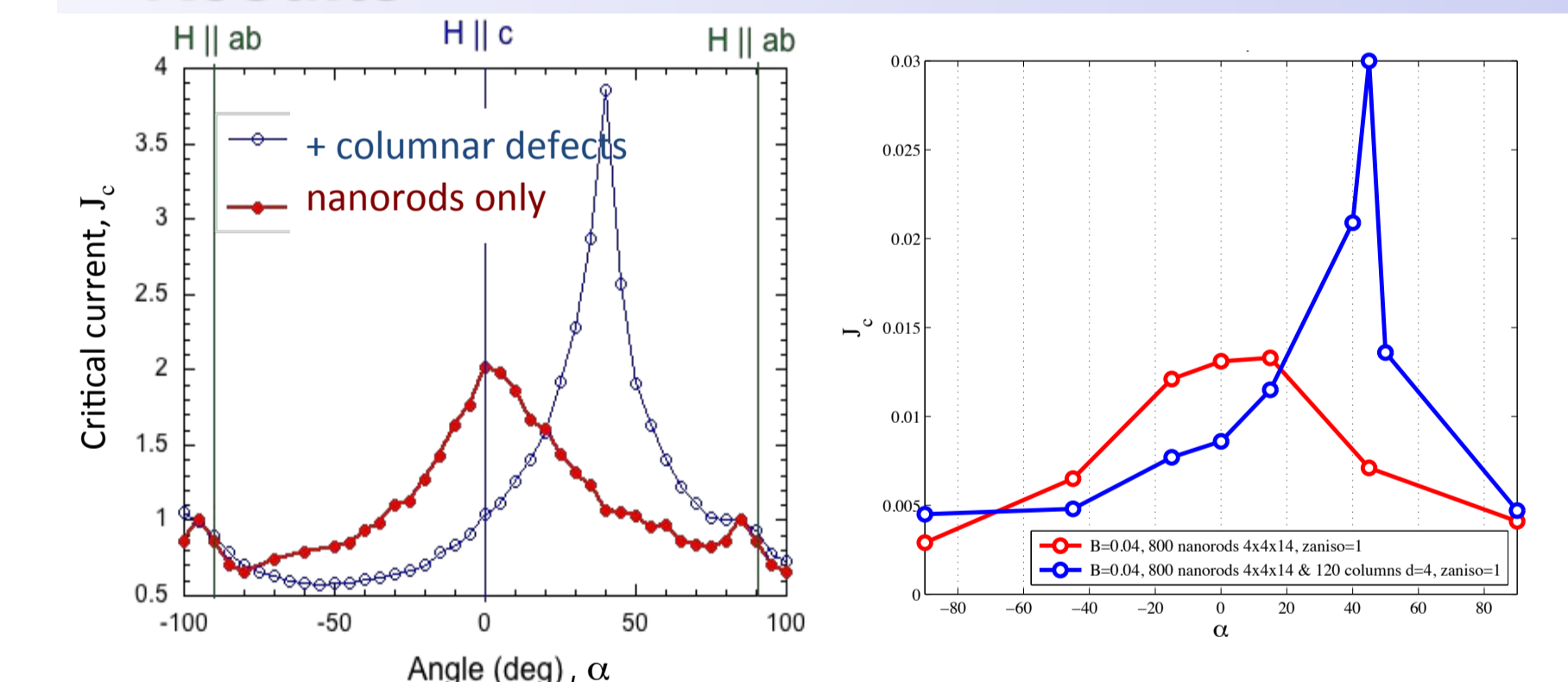
### Simulation



Two new extensions to the main simulations code required:

- Arbitrary external magnetic field direction
- Rotation-symmetric (cylindrical) integration domain

### Results



Left: Experimental J<sub>c</sub>( $\alpha$ ) dependence. Right: Numerical J<sub>c</sub>( $\alpha$ ) dependence. Red (nanorods) and blue (nanorods + columnar defects) lines are calculated slightly below the matching field of the system.

- The effects from different defects are not additive. Additional defects can simultaneously decrease the critical current at some directions of the magnetic field and increase it at other directions.
  - The alignment of the dominant inclusions define peaks. In case of nanorods the peak of J<sub>c</sub>( $\alpha$ ) is observed at  $\alpha = 0^\circ$  and in the case of dominating continuous columnar defects it is  $\alpha = 45^\circ$ .
  - The peak at  $\alpha = 0^\circ$  decreases. The critical current in systems with nanorods is larger than the one in the system with nanorods and columnar defects at  $\alpha = 0^\circ$ . In the former case it is obvious that the pinning is best as the defects a longest parallel to the vortices. On the other hand, continuous cylindrical inclusions allow vortices to move creating "rails" across the system.
- Close to quantitative agreement of experimental results and explanation of the underlying mesoscopic mechanisms

